DEPTH TO THE BOTTOM OF LITHOSPHERIC MAGNETIC SOURCES IN MONGOLIA

A.I. Filippova*, S.V. Filippov**

Pushkov Institute of Terrestrial Magnetism, Ionosphere, and Radio Wave Propagation of RAS (IZMIRAN), Moscow, Troitsk, Russia

**e-mail: aleirk@mail.ru*

***e-mail: sfilip@izmiran.ru*

Received September 30, 2024

Revised November 26, 2024

Accepted December 12, 2024

We estimate the depth to the bottom of lithospheric magnetic sources for the territory of Mongolia based on the global lithospheric magnetic field EMAG2v3 model using a centroid method. The obtained results are compared with independent geophysical data and a distribution of epicenters of regional earthquakes with M ≥ 5.0 for the observation period of 1900–2023. It has been found that the shallowest depths to the bottom of the lithospheric magnetoactive layer (<30 km) are seen predominantly under the mountain regions in Western and Central Mongolia and adjacent areas while the deepest bottom depths (>35 km) are observed to the east of 105° E. Therefore, the lithospheric magnetoactive layer is within the crust under the considered territory. A negative correlation between the Moho depth and the depth to the bottom of lithospheric magnetic sources is traced and there is a positive correlation between the lithospheric thickness and the depth to the bottom of lithospheric magnetic sources. We also demonstrate in this study that sources of the most earthquakes with M ≥ 6.0, recorded in 1900–2023, are nucleated in the areas in which a sharp change (>5 km) in the magneroactive layer thickness is observed.

Keywords: lithospheric geomagnetic field; centroid method; thermal regime of the lithosphere; seismicity; Mongolia

DOI: 10.31857/S00167940250310e4

1. INTRODUCTION

From a geological perspective, the territory of Mongolia is composed of different-aged terranes of various geodynamic origins [Gordienko et al., 2019; Yanshin, 1974; Tseden et al., 1992]. Folded and associated longitudinal fault structures form a system of gentle arcs open to the north. According to geophysical data, the study area (Fig. 1) is conventionally divided into three major regions: areas of intense mountain building in the west (Mongolian and Gobi Altai, Khangai uplift),

moderate mountain building in the central part (Khentei uplift), and weak mountain building in the south and east of the country [Zorin et al., 1982].

Fig. 1.

The main features of the deep structure of the lithosphere in the region under consideration are as follows. The mountain structures of the Mongolian Altai and Khangai uplift have the greatest thickness of the Earth's crust (about 50 km), while in the east of the country, the crust is significantly thinner - 37-40 km [Laske et al., 2013]. The lowest velocities of *P* -and *S* -waves are observed in the upper mantle beneath Khangai [Wu et al., 2021; Seredkina et al., 2016], where according to receiver function data, the asthenosphere roof is in close proximity to the base of the crust [Mordvinova et al., 2017]. The areas of weak mountain building in the south and east of Mongolia are characterized by greater lithosphere thickness (about 150 km) and higher seismic wave velocities in the upper mantle [Seredkina et al., 2017; Sloan et al., 2011]. The presence of anisotropic properties of the upper mantle material beneath the study area has been established both from surface wave data [Yanovskaya and Kozhevnikov, 2006; Seredkina and Solovey, 2018] and from SKS wave splitting (*S* -wave that passed through the mantle, propagated in the liquid core as a *P* -wave, and again as an *S* -wave in the mantle on its way to the receiver) [Barruol et al., 2008]. Based on statistical analysis of focal mechanisms of regional earthquakes, it has been established that the Earth's crust in the region is deformed under conditions of transpression (transitional regime from shear to compression) and shear regimes [Heidbach et al., 2018; Seredkina and Melnikova, 2018]. The orientation of compression axes changes from almost submeridional in the west of the area under consideration to northeastern in Central Mongolia. The same trends have been revealed by the results of observations of the deformation regimes of the Asian lithosphere using GPS geodesy methods [Lukhnev et al., 2010; Calais et al., 2003].

Analysis of the spatial morphology of the anomalous magnetic field over the territory of Mongolia, conducted in the works [Ayuushzhav et al., 1975; Blumentsvaig and Popov, 1977], allowed to identify a number of blocks and fault disruptions with certain characteristics of the magnetic field. For example, it was shown that the Bolnay fault is manifested as a zone with a large gradient of the magnetic field. The results of studies of the long-wavelength component of the anomalous magnetic field, performed using data from the CHAMP satellite at an altitude of about 290 km, allow conditionally dividing the region into two parts: in the western part (west of 100° E), predominantly positive magnetic field anomalies are observed, and in the eastern part – negative ones [Abramova et al., 2018]. Features of the geodynamic evolution of the lithosphere in the

considered area and its individual blocks are examined based on the generalization of paleomagnetic data in the work [Kovalenko et al., 2022].

The first estimates of the thickness of the magnetoactive layer of the lithosphere for the territory of Mongolia were made in the work [Zorin et al., 1982]. According to them, in the west of the country, the thickness was 16-25 km with an average value of 21 km, and in the east – 17-21 km with an average value of 19 km. However, in studies conducted in the last decade, it was shown that lithospheric magnetic sources in the region under consideration can lie at greater depths – up to 30-40 km [Gard and Hasterok, 2021; Tserendug et al., 2017]. At the same time, modern models obtained by various methods, for example, [Gard and Hasterok, 2021; Hou et al., 2024; Lei et al., 2024; Li et al., 2017], can also differ significantly from each other for individual regions of Mongolia (see section 4.1).

Due to the above-mentioned inconsistency in various estimates of the depth of the lower boundary of the magnetoactive layer of the lithosphere, this study aimed to obtain the distribution of this depth for the territory of Mongolia with high horizontal resolution based on the most modern model of the anomalous magnetic field EMAG2v3 [Meyer et al., 2017]. Analysis and verification of the results were carried out using independent geophysical data on the deep structure of the crust and upper mantle, surface heat flow, thermal water sources, and temperature models of the lithosphere (see sections 3 and 4.2). Additionally, in section 4.3, the obtained results are discussed in light of the seismicity characteristics of the region under consideration.

2. DATA AND METHODS

To determine the depths of lithospheric magnetic sources for the territory of Mongolia, we used the global model of the Earth's anomalous magnetic field EMAG2v3 [Meyer et al., 2017] (Fig. 2), reduced to a height of 4 km above sea level and having a horizontal resolution of 2 arc minutes. It should be noted that some rather extensive areas within the study region (Mongolian Altai, partially Khubsugul area and the central part of Khangai) were excluded from the analysis due to the absence of source data in EMAG2v3.

Fig. 2.

The calculations were carried out using the centroid method [Okubo et al., 1985; Tanaka et al., 1999]. The main assumption of the method is that the magnetization in a horizontally infinite layer is considered a random function of horizontal coordinates independent of depth. As for the region of Eastern Transbaikalia adjacent to Mongolia [Filippova et al., 2021], depth estimates were performed in square blocks with dimensions of 200×200 km. As was shown in [Filippova and Filippov, 2023a],

such a block size allows determining the lower boundary of the magnetoactive layer of the lithosphere without distortion to a depth of about 55 km. To improve the horizontal resolution of the obtained estimates, the overlap between adjacent blocks was 1° in latitude and 100 km in longitude. A total of 104 blocks covering the territory of Mongolia were processed, excluding areas not provided with source data. The central points of the blocks are shown in Fig. 2.

Azimuthally-averaged Fourier power spectra of geomagnetic field anomalies were calculated using the Fourpot 1.3b software [Pirttijärvi, 2015]. Following recommendations from [Núñez Demarco et al., 2021], preliminary data filtering and reduction to the pole were not performed.

Determination of depths of lithospheric magnetic sources – the center of mass (Z_0), upper (Z_t) and lower boundaries (Z_b) – was carried out using the obtained azimuthally-averaged Fourier power spectra of geomagnetic field anomalies according to the following relationships [Tanaka et al., 1999]:

$$ln\left[\Phi_{\Delta T}(|k|)^{1/2}/|k|\right] = lnA - |k|Z_0\ , \quad (1)$$

$$ln\left[\Phi_{\Delta T}(|k|)^{1/2}\right] = lnB - |k|Z_t\ , \quad (2)$$

$$Z_b = 2Z_0 - Z_t\ , \quad (3)$$

where $\Phi_{\Delta T}$ – azimuthally-averaged Fourier power spectrum of geomagnetic field anomalies; $|k| = \sqrt{k_x^2 + k_y^2}$ – modulus of the wave number; k_x and k_y – projections of the wave number along the **x** and **y** axes in the horizontal plane, *A, B* – constant values.

According to the results of synthetic tests from [Núñez Demarco et al., 2021], the wave number ranges in which we estimated the depths of the center of mass and the upper boundary of magnetic sources were ~0–0.05 rad/km (relationship (1)) and 0.25–0.50 rad/km (relationship (2)), respectively.

Depth determination errors (ε), not accounting for the error of the initial data, were calculated as in [Okubo and Matsunaga, 1994; Salazar et al., 2017]:

$$\varepsilon = \frac{\sigma}{|k_2| - |k_1|}\ , \quad (4)$$

where σ – standard deviation of the linear approximation from the observed spectrum; $|k_2|$ and $|k_1|$ – upper and lower boundaries of the wave number range in which the desired parameters were determined.

It should be noted that for the territory of Mongolia, the errors of the EMAG2v3 model are rather high – up to ~200 nT [Meyer et al., 2017]. However, as shown in [Seredkina, Filippov, 2021; Filippova et al., 2024], adding random noise with an amplitude of ±167 nT to the original data does

not lead to significant distortion of the depth values of the lower boundary of lithospheric magnetic sources, which is of primary interest for interpretation. At the same time, the difference in depth estimates Z_b with and without noise addition does not exceed the errors determined by equation (4).

3. RESULTS

As a result of the calculations, it was found that the depth of the upper boundary of lithospheric magnetic sources (Z_t) under the considered part of Mongolia varies from 0.2 to 3.8 km and has an average value of about 1.5 km. As in the case of the Baltic Shield [Filippova and Filippov, 2023a], the distribution of depth Z_t does not demonstrate certain patterns. This may partly be a consequence of rather large errors estimated using equation (4). Thus, their magnitude was 0.04-1.5 km with an average error value of ~0.5 km. In addition, the depth of the upper boundary of magnetic sources may be significantly distorted by errors in the source data [Seredkina and Filippov, 2021]. Finally, according to the global crustal structure model CRUST 1.0 [Laske et al., 2013], the sediment thickness throughout the entire region under consideration varies insignificantly – from their almost complete absence in the west to approximately 1 km in the east. Taking into account the difference in the magnetization of sedimentary rocks and crystalline basement rocks [Yanovsky, 1978], small variations in the thickness of the sedimentary layer may also contribute to the lack of patterns in the depth distribution Z_t.

The values we obtained for the depth of the center of mass of lithospheric magnetic sources (Z_0) vary approximately from 13 to 21 km, with an average of ~17 km. Variations of this depth have the same features as the distribution of the depth of the lower boundary of the magnetoactive layer (Z_b), shown in Fig. 3. This pattern, explicitly demonstrated for the East Siberian Sea [Filippova and Filippov, 2022], directly follows from relation (3) and small depth values of Z_t. The errors in determining Z_0 ranged from 0.3 to 3.0 km with an average value of about 1.9 km.

Fig. 3.

Variations in the depth of the lower boundary of lithospheric magnetic sources beneath the study region range approximately from 25 to 40 km (Fig. 3). The parameter reaches its minimum values (Z_b<30 km) predominantly beneath the mountainous areas of Western and Central Mongolia (Khangai and Khentei uplifts, Gobi Altai) and adjacent regions. It should be noted that for the central part of Khangai, estimates of Z_b were not obtained due to the lack of source data (Fig. 2). The deepest position of the lower boundary of the lithospheric magnetoactive layer (Z_b>35 km) is traced mainly east of 105° E. In addition, the Khubsugul region, the southern part of the Great Lakes Depression, and the eastern end of the Gobi Altai are characterized by local maxima of Z_b depth.

Based on the errors of depths Z_t and Z_0 estimated from relation (4), the error of depth Z_b is 0.4–4.7 km with an average value of about 3.2 km. Further, when comparing the features of the obtained distribution of the depth of the lower boundary of lithospheric magnetic sources with the field of epicenters of regional earthquakes, only variations of Z_b greater than 5 km, i.e., exceeding the maximum depth determination error, will be considered significant.

Taking into account the obtained errors and uncertainties in the Moho depth values in the global model CRUST 1.0 [Laske et al., 2013], the magnetoactive layer of the lithosphere within the considered territory is ubiquitously located in the Earth's crust (Fig. 3, 4). Overall, an inverse relationship can be identified between the Moho depths and Z_b - if the former decreases from west to east, the latter increases. Interestingly, the relationship between the depth of the lower boundary of lithospheric magnetic sources and lithospheric thickness is, on the contrary, direct. Thus, the thinnest lithosphere under the considered territory characterizes the mountainous regions in western Mongolia (Mongolian and Gobi Altai, Khangai), and to the east, the lithosphere-asthenosphere boundary gradually deepens [Seredkina et al., 2017; Seredkina et al., 2016; Sloan et al., 2011].

Fig. 4.

4. DISCUSSION

4.1. Comparison of results with other estimates of the depth of the lower boundary of lithospheric magnetic sources

Let us compare our results (Fig. 3) with independent estimates of the depth of the lower boundary of lithospheric magnetic sources from works [Gard and Hasterok, 2021; Hou et al., 2024; Lei et al., 2024; Li et al., 2017; Tserendug et al., 2017]. According to regional determinations of the depth Z_b obtained for the southwest of the Khentei uplift (Fig. 1) [Tserendug et al., 2017], it is 27-32 km for the area bounded approximately by 47.80°-48.05° N and 106.25°-106.65° E, and 30-33 km within 47.7°-48.0° N and 107.1°-107.4° E. Calculations were performed using the centroid method [Tanaka et al., 1999] based on data from areal geomagnetic surveys. Despite differences in the anomalous magnetic field models used and the significant difference in the sizes of the analyzed blocks, in our work, similar values of Z_b~33 km were obtained (Fig. 3).

For the Khangai and adjacent territories, global models of the distribution of the lower boundary depth of the lithosphere's magnetically active layer give similar estimates of about 25 km [Gard and Hasterok, 2021; Li et al., 2017], which also does not contradict our results, which unfortunately do not cover the central part of the uplift (Fig. 3). A slightly shallower occurrence Z_b – 16-22 km – was determined for this area in the work [Hou et al., 2024]. The same applies to the

Khentei uplift, which according to all mentioned models is characterized by a relatively shallow position of Z_b. The greatest differences are observed for the Khubsugul region and areas of weak mountain formation in the south and east of Mongolia. According to [Li et al., 2017; Hou et al., 2024], Z_b under these territories is only about 15-20 km, while the lower boundary of lithospheric magnetic sources lies significantly deeper according to data from [Gard and Hasterok, 2021] (approximately at 35 km) and our estimates (up to 35-40 km).

It is worth mentioning separately the results obtained in the work [Lei et al., 2024], which indicate an absolutely opposite nature of the depth distribution of Z_b under the considered territory relative to all other studies, including ours. Thus, the authors found that lithospheric magnetic sources lie deepest (38-48 km) under areas of intense mountain formation in western Mongolia and the Khangai uplift, and in the Khubsugul region they extend to a depth of about 30 km. At the same time, in the eastern part of the country, including the Khentei uplift, relatively small depths of Z_b are observed – from 20 to 30 km. Note that such a model of the depth distribution of Z_b does not agree with the results of independent geophysical studies discussed further (see section 4.2).

The reasons for the identified discrepancies between different models have been repeatedly discussed by us earlier [Filippova et al., 2021, 2024; Filippova and Filippov, 2022, 2023a, b, etc.] and, firstly, may be related to differences in the data used. For example, in [Li et al., 2017], the anomalous magnetic field was defined by the EMAG2v2 model [Maus et al., 2009], in [Gard and Hasterok, 2021] – by spherical harmonics of degree 16–100 of the LCS-1 model [Olsen et al., 2017], in [Hou et al., 2024] – by a new compilation of geomagnetic data from WDMAM2.1 (https://wdmam.org/), and in [Lei et al., 2024] – by a combination of EMM2017 models (https://www.ncei.noaa.gov/products/enhanced-magnetic-model) and EMAG2v3 [Meyer et al., 2017]. Secondly, the discussed results have somewhat different horizontal resolutions: 156 km in [Gard and Hasterok, 2021], 0.5×0.5° in [Lei et al., 2024], and about 100 km for our distribution (defined as the distance between the central points of adjacent blocks). Blocks of 300×300 km size and 100 km distance between the central points of adjacent blocks were used in [Hou et al., 2024]. It should be noted that determining the horizontal resolution of the model [Li et al., 2017] is difficult because it was obtained as the average value of the depth Z_b, determined in blocks of three different sizes – 98.8×98.8, 195.0×195.0, and 296.4×296.4 km. Finally, all discussed distributions of Z_b were obtained using different methods: in [Gard and Hasterok, 2021], the equivalent dipole method was used [Dyment and Arkani-Hamed, 1998]; in [Li et al., 2017; Hou et al., 2024] – the spectral method [Li and Wang, 2016], which takes into account the fractal distribution of magnetization in a layer uniformly magnetized with depth; in this paper – the centroid method [Tanaka et al., 1999]. Note

that in [Hou et al., 2024] the fractal parameter was not fixed as in [Li et al., 2017], but was estimated for each analyzed block. Inversion of magnetic data by the *equivalent source method* was performed in [Lei et al., 2024], with the magnetic susceptibility distribution model specified *a priori* , as in [Gard and Hasterok, 2021], which can serve as an additional source of errors.

4.2. Comparison of results with independent geophysical data

Based on the fact that the main magnetic mineral in the continental lithosphere is magnetite with a Curie point temperature of 578°C [Langel and Hinze, 1998], the distribution of the depth of the lower boundary of lithospheric magnetic sources obtained by us (Fig. 3) can be approximately considered as the distribution of the depth of the 578°C isotherm and compared with known data on the thermal regime of the lithosphere in the study area. The most direct information about deep temperatures, not distorted by initial assumptions and computational errors, is provided by the surface heat flow (q , mW/m^2). It should be noted that different regions of Mongolia are very unevenly provided with flow measurement points (Fig. 5 *a*) [Fuchs et al., 2021a, b]. Thus, only a few such points fall within the areas of intensive mountain building in the western and central parts of the country, as well as weak mountain building in the east. The submeridional area between 104°E and 113°E is best provided with surface heat flow measurements, where there is a tendency for flow values to increase in the northern direction - towards the Khentei uplift (Fig. 5 *a*). This is generally consistent with our results (Fig. 3), taking into account their coarser horizontal resolution relative to point determinations of flow. A large number of heat flow measurements were performed in loose sedimentary deposits of Lake Khubsugul [Khutorskoy et al., 1991]. Here, elevated values (more than 100 mW/m^2) of q are mainly observed (Fig. 5 *a*), which contradicts the relatively deep position of the depth Z_b that we obtained for the southern part of the Khubsugul region (Fig. 3). Such a discrepancy is most likely due not to a greater degree of lithosphere heating under the lake, but to overestimated flow values resulting from the redistribution of deep heat by groundwater, as shown for the Khubsugul and Baikal basins in [Golubev, 2007].

Fig. 5.

Certain ideas about the temperature regime of the lithosphere can be obtained not only from surface heat flow values but also from the analysis of hydrothermal data. A large number of thermal springs discharging at the surface are known in Mongolia (Fig. 5 *b*) [Tseesuren, 2001]. Notably, many of them are located in areas where no drilling has been conducted, i.e., there are no measurements of surface heat flow. Comparing our results with the spatial distribution of

geothermal springs, we note that most of the latter fall into areas of intense mountain building with a shallow occurrence of the lower boundary of lithospheric magnetic sources (Fig. 5 *b*).

According to the TC1 continental lithosphere temperature model [Artemieva, 2006], the depth of the 550°C isotherm beneath the study region varies approximately from 30 km in the western part of the country and under the Khentei uplift to 35-40 km in the east. With the exception of the Khubsugul region, where elevated temperatures in TC1 may be a consequence of overestimated heat flow values (see above) used in the model as input data, such temperature distribution fully corresponds to the deepening of Z_b in the eastern direction that we identified (Fig. 3). The same trend is also observed in the temperature distribution at a depth of 100 km, calculated in [Deng and Tesauro, 2016] for China and adjacent territories based on *S* -wave velocities [Li et al., 2013]. The surface-wave model from [Seredkina et al., 2017; Seredkina et al., 2016], which shows an increase in *S* -wave velocities in the upper mantle from west to east of Mongolia, is also consistent with the obtained results.

4.3. Seismicity and depth of the lower boundary of lithospheric magnetic sources

The territory of Mongolia is characterized by a fairly high level of seismic activity (Fig. 6). The most highly seismic areas are the zones of the Mongolian and Gobi Altai, the Ubsu-Nur lake region, the Bolnai zone, Mogod and Khubsugul area [Melnikova, Seredkina, 2017], while east of 105° E the number of strong earthquakes recorded during the instrumental observation period decreases sharply. Of greatest interest for comparison with our results are the depths of regional earthquake foci, which can be used to determine the lower boundary of the seismically active layer. It is believed that the temperature at this boundary reaches 300–400°C [Sibson, 1984], i.e., approximately corresponds to the depth of the center of mass of lithospheric magnetic sources [Filippova et al., 2021; Tanaka and Ishikawa, 2005]. In the region under consideration, the number of reliable (with known and low magnitude errors) determinations of hypocenter depths is small (see, for example, the ISC [Internarional..., 2024] and GCMT [Global..., 2024] catalogs), which makes it difficult to estimate the lower boundary of the seismically active layer. The tendency for regional earthquake depths to increase in the eastern direction, generally consistent with the deepening of the lower boundary of the magnetically active layer (Fig. 3), was revealed in the work [Sloan et al., 2011]. However, it was obtained based on the analysis of a small number of earthquakes and, therefore, requires confirmation on more representative source material.

In conclusion, let us compare our results with the distribution of epicenters of strong and moderate ($M \geq 5.0$) regional earthquakes recorded during the instrumental observation period,

including early instrumental data (since 1900). As shown in Fig. 6, the foci of most seismic events with $M \geq 6.0$ gravitate toward areas where there is a sharp change in the depth of Z_b. As mentioned earlier, only variations of Z_b greater than 5 km are considered significant, i.e., exceeding the maximum error in depth determination. The same relationship between variations in the depth of the lower boundary of lithospheric magnetic sources and the distribution of earthquake epicenters was previously identified by us for northeastern Eurasia [Filippova and Filippov, 2024]. Interestingly, in the eastern Khentei Highlands, which is also a zone with significant changes in the depth of Z_b, no earthquakes with $M \geq 6.0$ have been recorded during the instrumental observation period (Fig. 6). However, according to the results of seismogeological studies, seismogenic dislocations were discovered here (within the Upper Kerulen depression) that formed as a result of three paleoearthquakes that occurred during the Holocene, with a maximum estimated magnitude of 7.5 [Smekalin et al., 2016].

5. CONCLUSIONS

Based on the global model of the anomalous magnetic field EMAG2v3, using the centroid method, estimates of the depth of the lower boundary of lithospheric magnetic sources (Z_b) were performed for the territory of Mongolia, excluding the Mongolian Altai, part of the Khubsugul region, and the central part of Khangai, where model data are not available, i.e., a digital map of Z_b for the study area was constructed. The obtained results were compared with independent geophysical data and the distribution of regional earthquake epicenters with $M \geq 5.0$ (1900-2023). As a result, the following was shown.

1. Variations in depth Z_b under the studied region range from approximately 25 to 40 km. Minimum values ($Z_b < 30$ km) of the considered parameter are reached primarily under the mountainous areas of Western and Central Mongolia and adjacent regions. The deepest position of the lower boundary of the magnetically active layer of the lithosphere ($Z_b > 35$ km) is traced mainly east of 105° E.

2. The magnetically active layer of the lithosphere within the considered territory is located everywhere in the Earth's crust. At the same time, there is an inverse relationship between the Moho depths and Z_b – if the first decreases from west to east, the second increases. The relationship between the depth of Z_b and the thickness of the lithosphere, on the contrary, is direct: under mountainous areas in western Mongolia, characterized by thin lithosphere, a decrease in Z_b is observed; toward eastern Mongolia, the lithosphere-asthenosphere boundary gradually deepens and the value of Z_b also increases.

3. The foci of most earthquakes with $M \geq 6.0$, registered in 1900-2023, gravitate to areas where there is a sharp change in the depth of Z_b (more than 5 km), which is also confirmed by the epicenters of paleoearthquakes with a maximum magnitude of 7.5 in the east of the Khentei Highlands, where significant changes in the values of Z_b are observed.

FUNDING

The work was carried out within the framework of the State assignment and the nstitute of Terrestrial Magnetism, Ionosphere and Radio Wave Propagation .

CONFLICT OF INTEREST

The authors declare no conflict of interest.

DATA AVAILABILITY

The obtained distribution of the depth of the lower boundary of lithospheric magnetic sources in digital form is available upon request at *aleirk@mail.ru* .

REFERENCES

− *Abramova D.Yu., Abramova L.M., Varentsov I.M. Filippov S.V.* Morphology of regional magnetic anomalies of the Baikal rift zone and surrounding territories // Geophysical Research. Vol. 19. No. 4. pp. 31-45. 2018. https://doi.org/10.21455/gr2018.4-3

− *Ayuushzhav G., Byambaa Ch., Lugovenko V.N.* Main features of the anomalous magnetic field structure in Mongolia // Analysis of the spatiotemporal structure of the geomagnetic field. Moscow: Nauka. P. 201–209. 1975.

− *Blumentsvaig G.I., Popov A.I.* On the relationship between the magnetic field and the geological structure of Central Mongolia / Geophysical studies of the Siberian platform. Irkutsk: East Siberian Publishing House. P. 93–103. 1977.

− *Golubev V.A.* Conductive and convective heat transfer in the Baikal rift zone. Novosibirsk: Academic Publishing House "Geo", 222 p. 2007.

− *Gordienko I.V., Metelkin D.V., Vetluzhskikh L.I.* Structure of the Mongol-Okhotsk fold belt and the problem of identifying the Amur microcontinent // Geology and Geophysics. Vol. 60. No. 3. P. 318–341. 2019. https://doi.org/10.15372/GiG2019018

− *Zorin Yu.A., Novoselova M.R., Rogozhina V.A.* Deep structure of the MPR territory. Novosibirsk: Nauka, 93 p. 1982.

− *Kovalenko D.V., Yarmolyuk V.V., Kozlovsky A.M.* Paleomagnetism of the central part of the Central Asian fold belt (Tuva, Mongolia) // Reports of the Russian Academy of Sciences. Earth Sciences. Vol. 504. No. 1. P. 75–84. 2022. https://doi.org/10.31857/S2686739722050085

− *Lukhnev A.V., Sankov V.A., Miroshnichenko A.I., Ashurkov S.V., Calais E.* Rotations and deformations of the Earth's surface in the Baikal-Mongolian region according to GPS measurements // Geology and Geophysics. Vol. 51. No. 71. P. 1006–1017. 2010.

− *Melnikova V.I., Seredkina A.I.* Parameters of seismotectonic deformations of the Earth's crust in Mongolia according to earthquake focal mechanisms data // Dangerous geological processes and forecasting of natural emergencies in Central Mongolia. Ed. D.P. Gladkochub. Irkutsk: ISU Publishing House, P. 61–67. 2017.

− *Mordvinova V.V., Ulziibat M., Kobelev M.M., Khritova M.A., Kobeleva E.A., Batsaikhan Ts.* Velocity structure and azimuthal anisotropy of the Earth's crust and upper mantle of Mongolia based on body wave data // Dangerous geological processes and forecasting of natural emergencies in Central Mongolia. Ed. D.P. Gladkochub. Irkutsk: ISU Publishing House, P. 29–39. 2017.

− *Seredkina A.I., Kozhevnikov V.M., Solovey O.A.* Deep structure and anisotropic properties of the upper mantle of Mongolia based on Rayleigh and Love wave dispersion data // Hazardous geological processes and forecasting of natural emergencies in Central Mongolia. Ed. D.P. Gladkochub. Irkutsk: ISU Publishing House, P. 20–29. 2017.

− *Seredkina A.I., Solovey O.A.* Anisotropic properties of the upper mantle of Central Asia based on dispersion of group velocities of Rayleigh and Love waves // Geodynamics and Tectonophysics. Vol. 9. No. 2. P. 413–426. 2018. https://doi.org/10.5800/GT-2018-9-2-0354

− *Seredkina A.I., Filippov S.V.* Depths of magnetic sources in the Arctic and their relationship with lithosphere parameters // Geology and Geophysics. Vol. 62. No. 7. P. 902–916. 2021. https://doi.org/10.15372/GiG2020162

− *Smekalin O.P., Chipizubov A.V., Imaev V.S.* Seismogeology of the Upper Kerulen basin (Khentei, Northern Mongolia) // Geodynamics and Tectonophysics. Vol. 7. No. 1. P. 39–57. 2016. https://doi.org/10.5800/GT-2016-7-1-0196

− *Filippova A.I., Filippov S.V.* Depths of lithospheric magnetic sources and thermal regime of the lithosphere under the East Siberian Sea // Physics of the Earth. No. 4. P. 71–84. 2022. https://doi.org/10.31857/S0002333722040032

− *Filippova A.I., Filippov S.V.* Depths of lithospheric magnetic sources under the Baltic Shield // Geomagnetism and Aeronomy. Vol. 63. No. 5. P. 667–679. 2023a. https://doi.org/10.31857/S0016794023600059

− *Filippova A.I., Filippov S.V.* Thermal regime of the lithosphere under the Taimyr Peninsula based on geomagnetic data // Geomagnetism and Aeronomy. Vol. 63. No. 3. P. 391–402. 2023b. https://doi.org/10.31857/S0016794022600600

− *Filippova A.I., Filippov S.V.* Depth of the lower boundary of lithospheric magnetic sources in northeastern Eurasia: thermal regime of the lithosphere and relationship with seismicity // Geomagnetism and Aeronomy. 2024. Vol. 64. No. 1. P. 149–160. https://doi.org/10.31857/S0016794024010155

− *Khutorskoy M.D., Golubev V.A., Kozlovtseva S.V., Mitnik M.M., Yarmolyuk V.V.* Thermal regime of the MPR subsurface. Moscow: Nauka, 127 p. 1991.

− *Yanovsky B.M.* Earth's magnetism. L.: Leningrad University. 592 p. 1978.

− *Yanovskaya T.B., Kozhevnikov V.M.* Anisotropy of the upper mantle of the Asian continent based on group velocities of Rayleigh and Love waves // Geology and Geophysics. Vol. 47. № 5. P. 622–629. 2006.

− *Yanshin A.L.* Tectonics of the Mongolian People's Republic. Moscow: Nauka, 283 p. 1974.

− *Artemieva I.M.* Global 1°×1° thermal model TC1 for the continental lithosphere: Implications for lithosphere secular evolution // Tectonophysics. V. 416. P. 245–277. 2006. https://doi.org/10.1016/j.tecto.2005.11.022

− *Barruol G., Deschamps A., Déverchère J., Mordvinova V., Ulziibat M., Perrot J., Artemiev A., Dugarmaa T., Bokelmann G.* Upper mantle flow beneath and around the Hangay dome, Central Mongolia // Earth Planet. Sci. Lett. V. 274. P. 221–233. 2008. https://doi.org/10.1016/epsl.2008.07.027

− *Calais E., Vergnolle M., San'kov V., Lukhnev A., Miroshnichenko A., Amarjargal S., Déverchère J.* GPS measurements of crustal deformation in the Baikal-Mongolia area (1994–2002): implications for current kinematics of Asia // J. Geophys. Res. V. 108. 2501. 2003. https://doi.org/10.1029/2002JB002373

− *Deng Y., Tesauro M.* Lithospheric strength variations in Mainland China: Tectonic implications // Tectonics. V. 35. P. 2313–2333. 2016. https://doi.org/10.1002/2016TC004272

− *Dyment J., Arkani-Hamed J.* Equivalent source magnetic dipoles revisited // Geophys. Res. Lett. V. 25. № 11. P. 2003–2006. 1998. https://doi.org/10.1029/98GL51331

– *Filippova A.I., Golubev V.A., Filippov S.V.* Curie point depth and thermal state of the lithosphere beneath the northeastern flank of the Baikal rift zone and adjacent areas // Surv. Geophys. V. 42. № 5. P. 1143–1170. 2021. https://doi.org/10.1007/s10712-021-09651-7

– *Filippova A.I., Filippov S.V., Radziminovich Ya. B.* Thermal state of the lithosphere beneath the Laptev Sea: Geodynamic implications from geomagnetic data // J. Asian Earth Sci. V. 261. 105970. 2024. https://doi.org/10.1016/j.jseaes.2023.105970

– *Fuchs S.; Norden B., Artemieva I. et al.* The Global Heat Flow Data-base: Release 2021. GFZ Data Services. 2021a. https://doi.org/10.5880/fidgeo.2021.014

– *Fuchs S., Beardsmore G., Chiozzi P. et al.* A new database structure for the IHFC Global Heat Flow Database // International Journal of Terrestrial Heat Flow and Applied Geothermics. V. 4. №. 1. P. 1–14. 2021b. https://doi.org/10.31214/ijthfa.v4i1.62

– *Gard M., Hasterok D.* A global Curie depth model utilizing the equivalent source magnetic dipole method // Phys. Earth Planet. Inter. V. 313. 106672. 2021. https://doi.org/10.1016/j.pepi.2021.106672

– Global CMT Web Page. 2024. On-line Catalog. Lamont-Doherty Earth Observatory (LDEO) of Columbia University, Columbia, SC, USA. Available from http://www.globalcmt.org. Last accessed 19 September 2024.

– *Heidbach O., Rajabi M., Cui X. et al.* The World Stress Map database release 2016: Crustal stress pattern across scales // Tectonophysics. V. 744. P. 484–498. 2018. https://doi.org/10.1016/j.tecto.2018.07.007

– *Hou J., Fang J., Wang K.* The Curie surface and lithospheric thermal structure in Mongolia-Baikal region // Journal of Geophysical Research: Solid Earth. V. 129. e2024JB028778. 2024. https://doi.org/10.1029/2024JB028778

– International Seismological Centre. 2024. On-line Bulletin. Internatl. Seis. Cent., Thatcham, United Kingdom. Available from http://www.isc.ac.uk. Last accessed 19 September 2024.

– *Langel R.A., Hinze W.J.* The magnetic field of the Earth's lithosphere. Cambridge University, Cambridge, UK. 450 p. 1998.

− *Laske G., Masters G., Ma Z., Pasyanos M.* Update on CRUST1.0 − A 1-degree global model of Earth's crust / Abstracts European Geoscience Union General Assembly. Vienna, Austria, 7–12 April, 2013. № EGU2013-2658. 2013.

− *Lei Y., Jiao L., Huang Q., Tu J.* A continental model of Curie Point Depth for China and surroundings based on Equivalent Source Method // Journal of Geophysical Research: Solid Earth. V. 129. e2023JB027254. 2024. https://doi.org/10.1029/2023JB027254

− *Li, C.-F., Wang, J.* Variations in Moho and Curie depths and heat flow in Eastern and Southeastern Asia // Mar. Geophys. Res. V. 37. № 1. P. 1–20. 2016. https://doi.org/10.1007/s11001-016-9265-4

− *Li Y., Wu Q., Pan J., Zhang F., Yu D.* An upper-mantle S-wave velocity model for East Asia from Rayleigh wave tomography // Earth Planet. Sci. Lett. V. 377. P. 367–377. 2013. https://doi.org/10.1016/j.epsl.2013.06.033

− *Li C.-F., Lu Y., Wang J.* A global reference model of Curie-point depths based on EMAG2 // Sci. Rep.V. 7. 45129. 2017. https://doi.org/10.1038/srep45129

– *Maus, S., Barckhausen U., Berkenbosch H. et al.* EMAG2: A 2-arc-minute resolution Earth Magnetic Anomaly Grid compiled from satellite, airborne and marine magnetic measurements // Geochem. Geophys. Geosyst. V. 10. Q08005. 2009. https://doi.org/10.1029/2009GC002471

– *Meyer B., Chulliat A., Saltus R.* Derivation and error analysis of the earth magnetic anomaly grid at 2 arc min resolution version 3 (EMAG2v3) // Geochem. Geophys. Geosyst. V. 18. P. 4522–4537. 2017. https://doi.org/10.1002/2017GC007280

– NOAA National Centers for Environmental Information. 2022: ETOPO 2022 15 Arc-Second Global Relief Model . https://doi.org/10.25921/fd45-gt74 . Available from https://www.ncei.noaa.gov/products/etopo-global-relief-model. Last accessed 19 September 2024.

– *Núñez Demarco P., Prezzi C., Sánchez Bettucci L.* Review of Curie point depth determination through different spectral methods applied to magnetic data // Geophys. J. Int. V. 224. № 1. P. 17–39. 2021. https://doi.org/10.1093/gji/ggaa361

− *Okubo Y., Graf R.J., Hansen R.O., Ogawa K., Tsu H.* Curie point depths of the island of Kyushu and surrounding areas, Japan // Geophysics. V. 50. P. 481–494. 1985.

− *Okubo Y., Matsunaga T.* Curie point depth in northeast Japan and its correlation with regional thermal structure and seismicity // J. Geophys. Res. V. 99. № B11. P. 22363–22371. 1994.

− *Olsen N., Ravat D., Finlay C.C., Kother L.K.* LCS-1: a high-resolution global model of the lithospheric magnetic field derived from CHAMP and Swarm satellite observations // Geophys. J. Int. V. 211. № 3. P. 1461–1477. 2017. https://doi.org/10.1093/gji/ggx381

− *Pirttijärvi M.* 2D Fourier domain operations, FOURPOT program. 2015. https://wiki.oulu.fi/x/0oU7AQ/

− *Salazar J. M., Vargas C.A., Leon H.* Curie point depth in the SW Caribbean using the radially averaged spectra of magnetic anomalies // Tectonophysics. V. 694. P. 400–413. 2017. https://doi.org/10.1016/j.tecto.2016.11.023

− *Seredkina A., Kozhevnikov V., Melnikova V., Solovey O.* Seismicity and S-wave velocity structure of the crust and the upper mantle in the Baikal rift and adjacent regions// Phys. Earth Planet. Inter. V. 261. P. 152–160. 2016. http://dx.doi.org/10.1016/j.pepi.2016.10.011

− *Seredkina A.I., Melnikova V.I.* Seismotectonic crustal strains of the Mongol-Baikal seismic belt from seismological data / Moment tensor solutions. Ed. S. D'Amico. Springer, Cham. P. 497–517. 2018. https://doi.org/10.1007/978-3-319-77359-9_22

− *Sibson R.H.* Roughness at the base of the seismogenic zone: contributing factors // J. Geophys. Res.: Solid Earth. V. 89. № B7. P. 5791–5799. 1984. https://doi.org/10.1029/JB089iB07p05791

− *Tanaka A., Ishikawa Y.* Crustal thermal regime inferred from magnetic anomaly data and its relationship to seismogenic layer thickness: The Japanese islands case study // Phys. Earth Planet. Inter. V. 152. P. 257–266. 2005. https://doi.org/10.1016/j.pepi.2005.04.011

− *Tseden T., Murao S., Dorjgotov D.* Introduction to geology of Mongolia // Bulletin of the Geological Survey of Japan. V. 43. № 12. P. 735–744. 1992.

− *Tseesuren B.* Geothermal resources in Mongolia and potential uses / Geothermal Training Programme, Iceland. P. 347–374. 2001.

− *Tserendug Sh., Bayanjargal G., Mungunshagai M.* The heat flows via CPD / Book of extended abstracts. The International Conference on Astronomy and Geophysics in Mongolia. Ulaanbaatatar, Mongolia, 20–22 July 2017. P. 74–78. 2017.

− *Sloan R.A., Jackson J.A., McKenzie D., Priestley K.* Earthquake depth distributions in central Asia, and their relations with lithosphere thickness, shortening and extension // Geophys. J. Int. V. 185. № 1. P. 1–29. 2011. https://doi.org/10.1111/j.1365-246X.2010.04882.x

− *Tanaka A., Okubo Y., Matsubayashi O.* Curie point depth based on spectrum analysis of the magnetic anomaly data in East and Southeast Asia // Tectonophysics. V. 306. P. 461–470. 1999.

− *Wu H., Huang Z., Zhao D.* Deep structure beneath the southwestern flank of the Baikal rift zone and adjacent areas // Phys. Earth Planet. Inter. V. 310. 106616. 2021. https://doi.org/10.1016/j.pepi. 2020. 106616

Figure Captions

Fig. 1. Study area. Topography (h , m - height above sea level) is shown according to the global model ETOPO 2022 [NOAA..., 2022]. Rectangles indicate the areas considered in the work [Tserendug et al., 2017].

Fig. 2. Modulus of the total vector of the anomalous geomagnetic field (T_a, nT) at a height of 4 km above sea level over the study area according to the EMAG2v3 model [Meyer et al., 2017] and the central points of 200 x 200 km blocks (white circles), within which calculations of the depths of lithospheric magnetic sources were performed.

Fig. 3. Depth of the lower boundary of lithospheric magnetic sources (Z_b, km).

Fig. 4. Moho depth (H , km) according to the global model CRUST 1.0 [Laske et al., 2013].

Fig. 5. Surface heat flow (q , mW/m^2) according to [Fuchs et al., 2021a] (a) and thermal water sources with maximum temperature indication (T , °C) according to [Tseesuren, 2001] (b) in comparison with our obtained distribution of the depth of the lower boundary of lithospheric magnetic sources (Z_b, km).

Fig. 6. Epicenters of regional earthquakes with $M \geq 5.0$, registered in 1900-1950 (gray circles) and 1950-2023 inclusive (white circles) according to the ISC catalog [International..., 2024] in comparison with our obtained distribution of the depth of the lower boundary of lithospheric magnetic sources (Z_b, km).

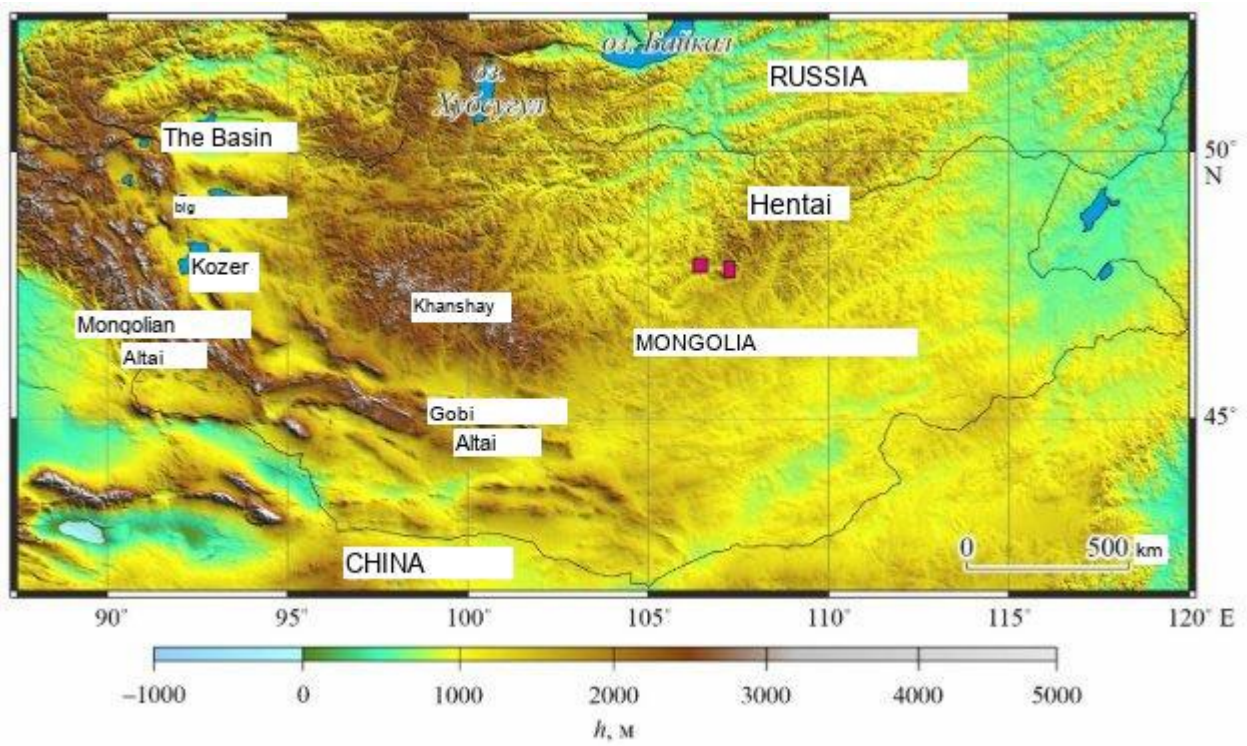
RUSSIA
The Basin
Hentai
Kozer
Khanshay
Monqolian
Altai
MONGOLIA
Gobi
Altai
CHINA
оз. Байкал
оз. Хубсугул
50° N
45°
0
500 km
90°
95°
100°
105°
110°
115°
120° E
−1000
0
1000
2000
3000
4000
5000
h, м

Fig. 1.

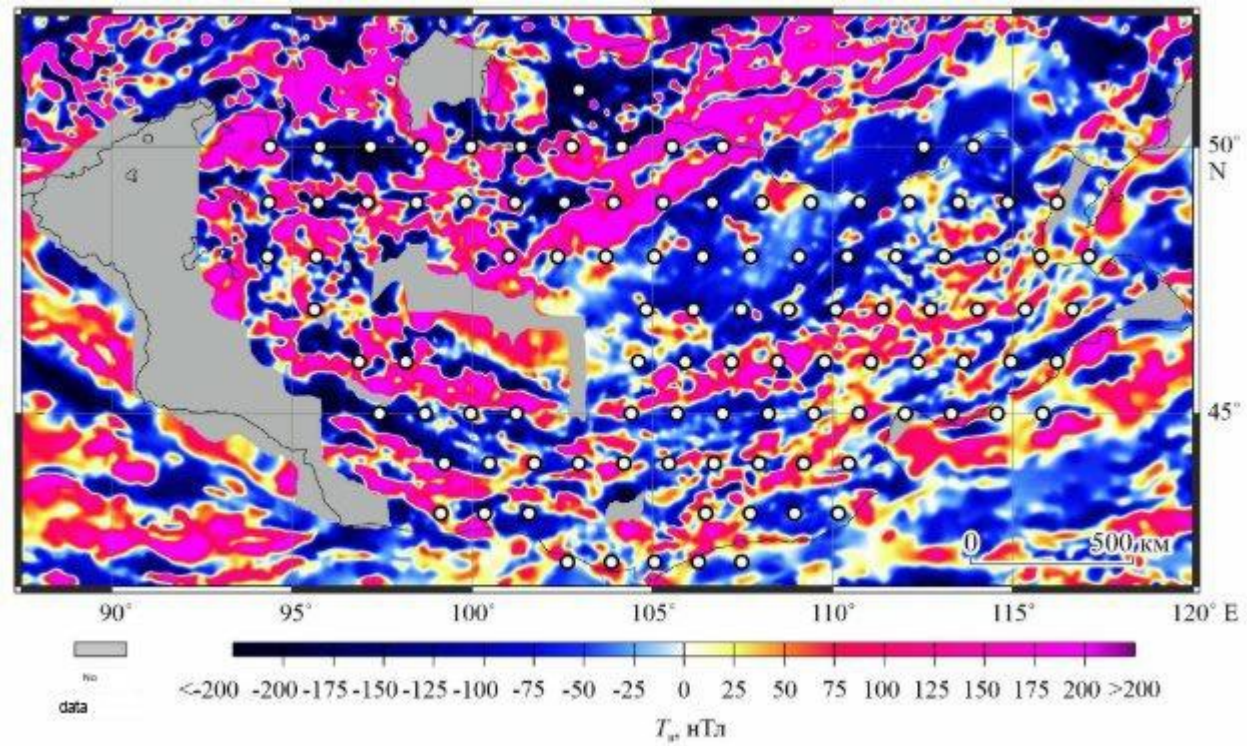
50° N
45°
0
500 км
90°
95°
100°
105°
110°
115°
120° E
No data
<-200 -200 -175 -150 -125 -100 -75 -50 -25 0 25 50 75 100 125 150 175 200 >200
T_a, нТл

Fig. 2.

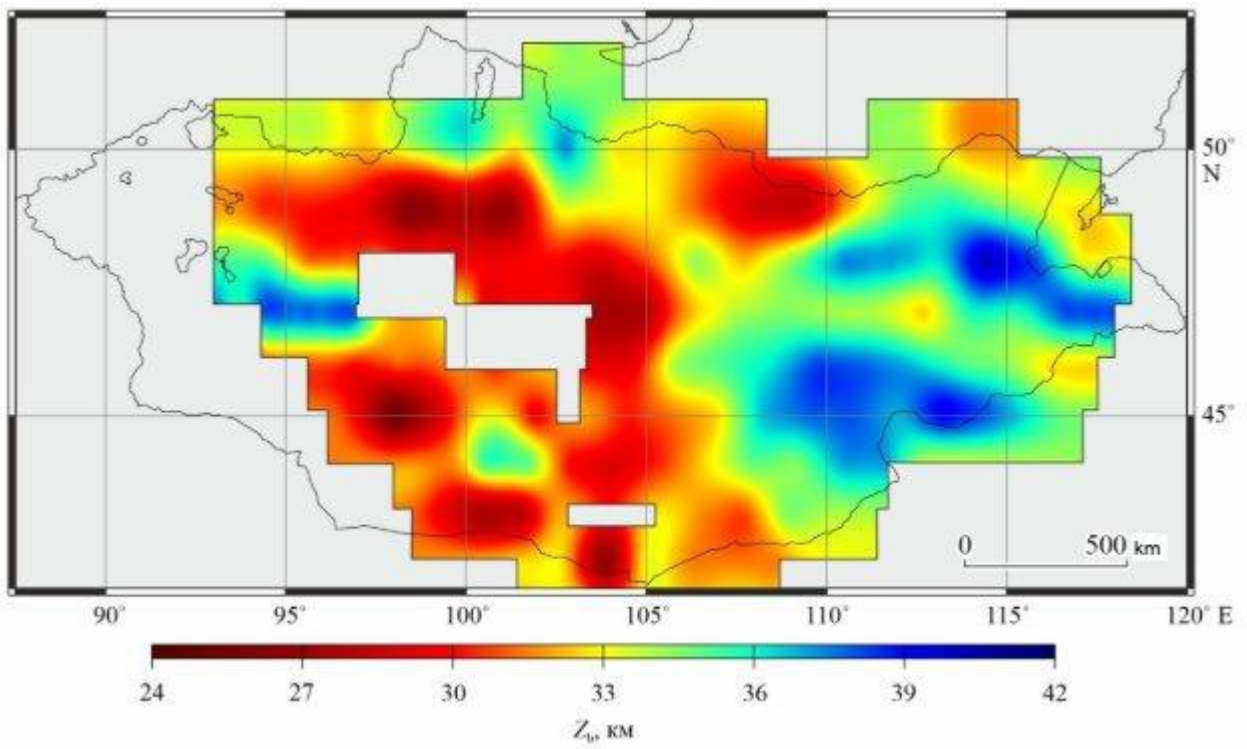
50° N
45°
0
500 km
90°
95°
100°
105°
110°
115°
120° E
24
27
30
33
36
39
42
Z_{tr}, км

Fig. 3.

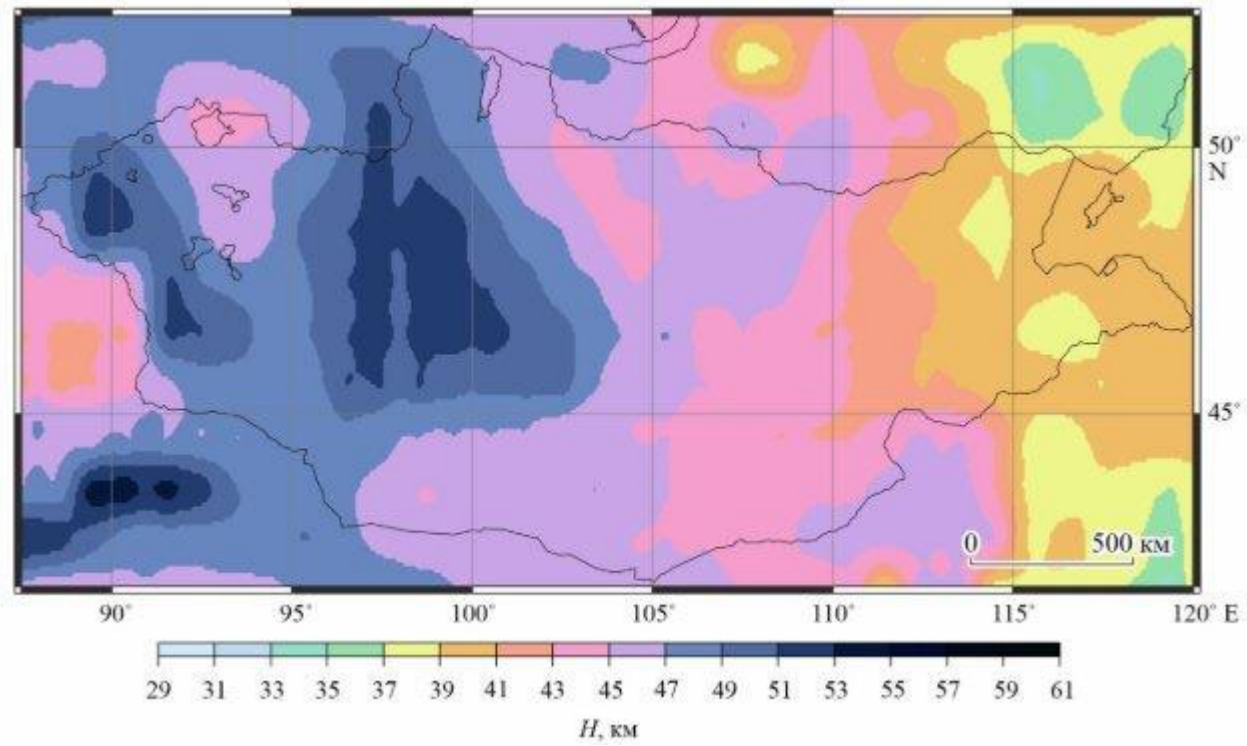
50° N
45°
0
500 км
90°
95°
100°
105°
110°
115°
120° E
29
31
33
35
37
39
41
43
45
47
49
51
53
55
57
59
61
H, км

Fig. 4.

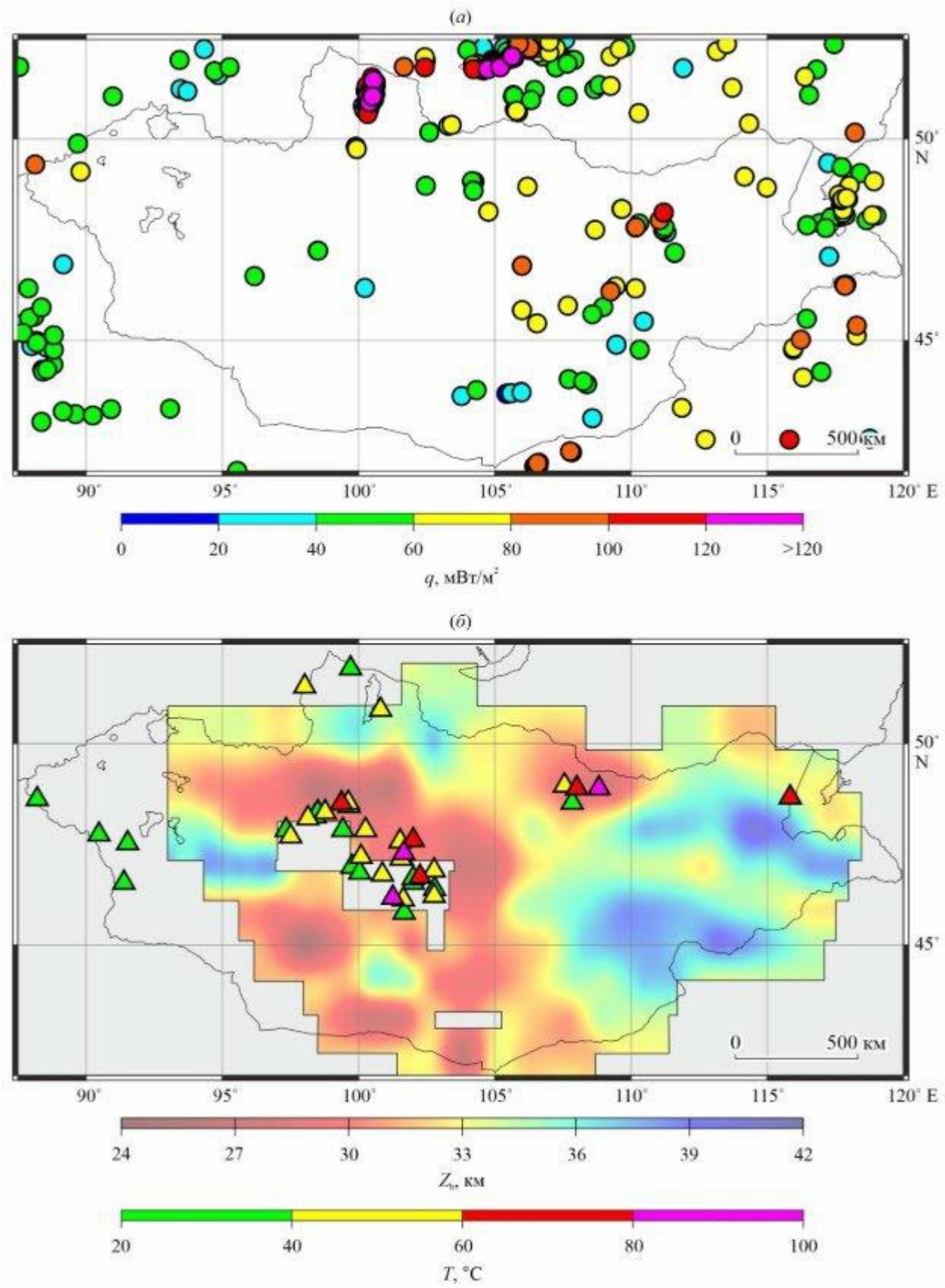
(а)
50° N
45°
0
500 км
90°
95°
100°
105°
110°
115°
120° E
0
20
40
60
80
100
120
>120
q, мВт/м²
(б)
50° N
45°
0
500 км
90°
95°
100°
105°
110°
115°
120° E
24
27
30
33
36
39
42
Z_b, км
20
40
60
80
100
T, °C

Fig. 5.

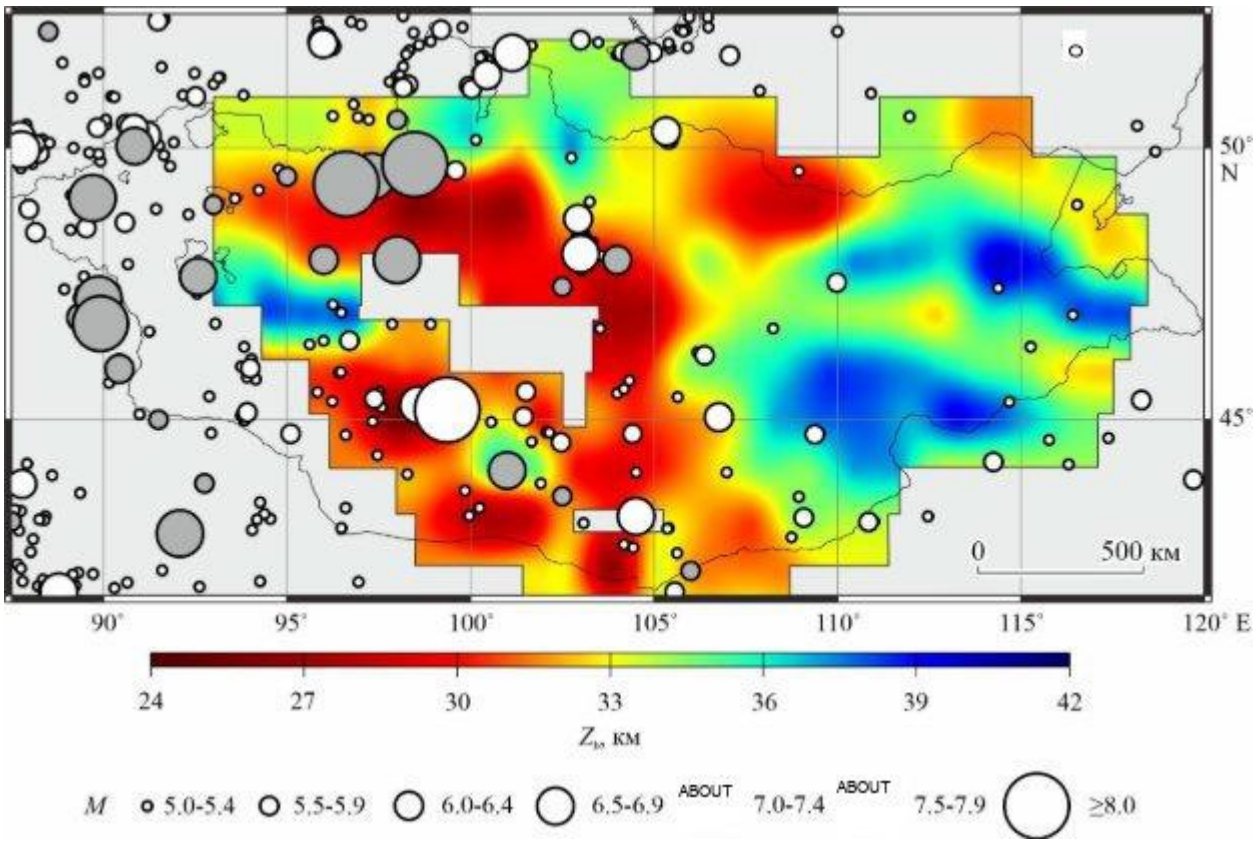
50° N
45°
0
500 км
90°
95°
100°
105°
110°
115°
120° E
24
27
30
33
36
39
42
Z_h, км
M
5.0-5.4
5.5-5.9
6.0-6.4
6.5-6.9
ABOUT
7.0-7.4
ABOUT
7.5-7.9
≥8.0

Fig. 6.